



Parametric study of the load-bearing mechanisms in RC beam-grids to resist progressive collapse

Didier Droogné

Phd student

Ghent University, Department of Structural Engineering

Ghent, Belgium
didier.droogne@ugent.be

Wouter Botte

Post-doctoral researcher

Ghent University, Department of Structural Engineering

Ghent, Belgium
wouter.botte@ugent.be

Robby Caspeele

Professor

Ghent University, Department of Structural Engineering

Ghent, Belgium
robby.caspeele@ugent.be

Contact: didier.droogne@ugent.be

1 Abstract

Recently, several structural failures demonstrated the disastrous consequences of progressive collapse and raised the awareness of the engineering community. However the low probability of progressive collapse makes it uneconomical to design every building against progressive collapse using conventional design methods. Furthermore in most cases the initiating events of progressive collapses are unknown during the design. As such, consideration of secondary load-carrying mechanisms can be an effective alternative. These mechanisms include compressive arch action (CAA) and tensile catenary action (TCA) in reinforced concrete (RC) beams. Several researchers have investigated the effects of CAA and TCA experimentally and numerically in individual RC beams. However to date limited studies have been carried out to study these mechanisms in RC beam-grids. Hence in this contribution a validated numerical model is developed to study and quantify the individual contributions and development of the different mechanisms in RC beam-grids. Parametric studies are performed in relation to the influence of the aspect ratio of the grid, reinforcement ratio and ultimate reinforcement strain.

Keywords: RC beam-grids, parametric study, progressive collapse, membrane action.

2 Introduction

Despite many significant theoretical and technological developments in the last decades, one unfortunately has to realize that structural robustness is still an issue of controversy. In this context several structural failures such as the collapse at Ronan Point (London 1968) and the WTC towers (New York 2001) demonstrated the disastrous consequences of progressive collapse and raised the awareness of the engineering community to design for structural robustness [1], [2]. Moreover recent construction techniques allow to build and design structures with minimal material consumption to optimize costs and

contemporary architectural trends require the use of high-performance materials which lead to light and flexible structures. However these tendencies result in a smaller inherent redundancy in the structure and a larger vulnerability to loading situations outside the design envelope. Hence, to avoid the high consequences related to progressive collapse structural robustness should be incorporated in the design of new buildings. Taking into account the low probability of progressive collapse using conventional design methods, it is uneconomical to design every building against progressive collapse. Furthermore in most cases the initiating events of progressive collapses are unknown during the design. As a consequence one of the common strategies to increase structural

robustness is the provision of alternate load paths. These alternate load paths increase the continuity and structural redundancy within the structure and allow a redistribution of loads to limit the damage extent in case of some local failure.

Based on numerous recent experimental findings and numerical studies on individual reinforced concrete beams and slabs, it is clear that these elements have a large potential to develop alternate load paths in RC structures due to the development of compressive or tensile membrane action [3]–[6]. For non-slender elements this compressive (CMA) and tensile membrane action (TMA) are often denoted as compressive arching action (CAA) and tensile catenary action (TCA). Despite the diverse tests on individual beams, up to date limited experimental and numerical studies have been carried out to study the mechanisms of compressive and tensile membrane action in reinforced concrete beam-grids consisting of orthogonally placed beams. Qian et al. [7] tested two scaled reinforced concrete beam-grids to compare the load bearing capacity of the isolated beam-grid to the load bearing capacity of the beam-grid combined with a reinforced concrete slab. Similarly Lu et al. [8] compared the load bearing capacity of a plain beam-grid to a beam-grid combined with a slab. However in the latter study, the beams and slab were only supported in one direction. Hence the beneficial three dimensional effect of the beam-grid could not be activated in that study.

When an orthogonal reinforced concrete beam-grid is subjected to the removal of a central support, the loads acting on the grid will in general have to be redistributed by the beams in both directions. Subsequently, membrane action will develop in the orthogonal beams due to the large deformations and interactions will occur between the different load bearing mechanisms of the elements. Considering the limited experimental results, the structural interactions and load redistribution between the different mechanisms are however still unclear. As experimental tests are more expensive and time-consuming, in this paper numerical studies are performed to study and quantify the individual contributions of the load bearing mechanisms found in general reinforced concrete beam-grids subjected to the notional

removal of a central support. The notional removal of a central support is chosen as an accidental state to obtain an objective and event-independent assessment of the resistance against progressive collapse. For each numerical study, the beam-grid consists of two orthogonally placed beams which are clamped at their supports and are intersecting at mid-span (Figure 1).

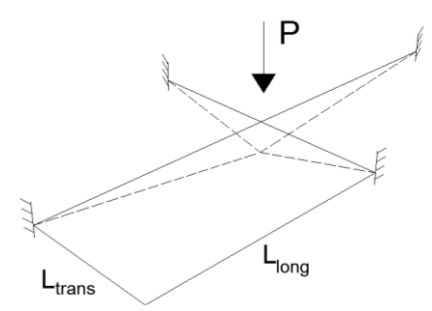


Figure 1. Reinforced concrete beam-grid subjected to a central support removal

Parametric studies are performed in relation to the influence of the aspect ratio of the grid, the reinforcement ratio, the slenderness of the beams and the reinforcement properties.

3 Numerical model

To perform the numerical studies in this contribution, the open-source software OpenSees is used [9]. This software was originally developed to model the behavior of structures under seismic actions and recently it has been applied in several studies to investigate progressive collapse [10], [11]. In the following the main modelling parameters and assumptions are summarized.

In order to reduce the computational effort, fiber elements with 6 degrees of freedom are used in the numerical model instead of solid elements. As such, taking into account the recommendations of Arshian [12], each beam is subdivided in 11 displacement-based fiber elements over its initial length which each have 3 Gauss-Legendre integration points. Geometrical nonlinearity is accounted for by implementing a co-rotational transformation. Further, nonlinear material behavior is also considered. As such for the concrete material, the 'concrete02' model is used which includes linear softening in tension and compression ($f_{c,residual}=0.20f_c$) [9]. Regarding the reinforcing steel, the 'steel02' model is used which

includes a plastic hardening phase [9]. For the solution algorithm Newton-Raphson is used in combination with ‘Broyden’ and ‘NewtonLineSearch’ to overcome convergence issues.

As illustrated in Figure 2, this fibre-based model has been validated to simulate the load-deflection behavior of orthogonal reinforced concrete beam-grids based on the experimental tests by Qian et al. [7]. Further note that similar to the experimental tests, in this investigation the beam-grid is subjected to a point-load at mid-span and is not loaded by uniform loads due to software limitations. As such it is not possible with the software OpenSees to account for large deformations combined with uniform loads in three dimensions using the co-rotational transformation. Nonetheless the observations and conclusions of this investigation can be generalized to uniform load scenarios (which are more representative regarding real situations). To limit the influencing factors of this study, the end supports of the beam are assumed as fully clamped. As discussed in [13], restraining the axial elongation of RC members will greatly enhance the development of membrane action.

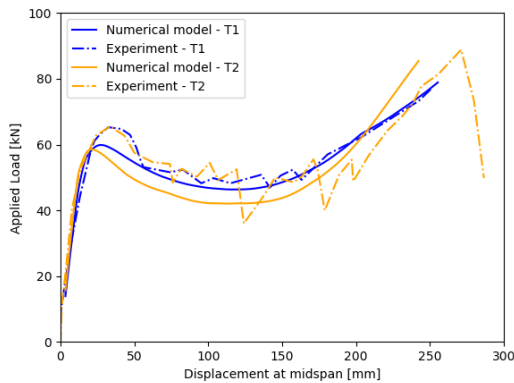


Figure 2. Comparison numerical model and experimental results of Qian et al. (2014).

4 Case study

As a reference model, a beam-grid is considered for which the length of the longitudinal beam in the initial situation, i.e. before the notional removal of the central support, is kept equal to 6 m. In the damaged situation this beam length doubles to 12 m. The height and width of the longitudinal beam are defined by the following equations:

$$h_{long} = l_{long,init.}/\lambda_{long} \tag{1}$$

$$b_{long} = 0.8 \cdot h_{long} \tag{2}$$

with λ_{long} the slenderness of the longitudinal beam in the initial situation and $l_{long,initial}$ the initial length of the longitudinal beam. The initial length of the transversal beam depends on the considered aspect ratio γ of the beam-grid:

$$l_{trans,init.} = \gamma \cdot l_{long,init.} \tag{3}$$

Next two approaches are chosen to investigate the influence of the aspect ratio γ on the development of membrane action in the beam-grids. In a first approach the slenderness of both orthogonal beams is kept equal while changing the aspect ratio of the beam-grid. In the second approach on the other hand, the height of both orthogonal beams is kept constant:

$$\lambda_{long} = \lambda_{trans}$$

Approach 1: or (3)

$$h_{long} = \gamma \cdot h_{trans}$$

Approach 2: $h_{long} = h_{trans}$ (4)

For both approaches the width b_{trans} of the transversal beam is equal to 0.8 times the height h_{trans} . The reinforcement ratio ρ of the reference model is kept equal to 0.01 for the longitudinal beam and transversal beam. The concrete cover of all beams is 25 mm. Further the reference model considers a concrete strength of 38 MPa and steel reinforcement characterized by a yield strength of 555 MPa, a strain-hardening ratio of 0.001 and an ultimate strain ϵ_{su} of 9.18 %. The latter corresponds to the mean value of the ultimate strain of the highest ductility class for reinforcement steel considered in EN1992-1-1 [14].

5 Results of case study for an aspect ratio γ of 0.5

In the left part of Figure 3 the load-deflection behavior up to failure of the reference beam-grid is shown for an aspect ratio γ of 0.5 and a relative slenderness of 12 for both the longitudinal and transversal beam. Note that failure in this study is defined by rupture of the reinforcement in the beam-grid. In order to quantify the load redistribution in the beam-grid between the

longitudinal and transversal beam, both beams are analyzed separately. The load-deflection behavior of the individual longitudinal and transversal beam is illustrated in the left part of Figure 3.

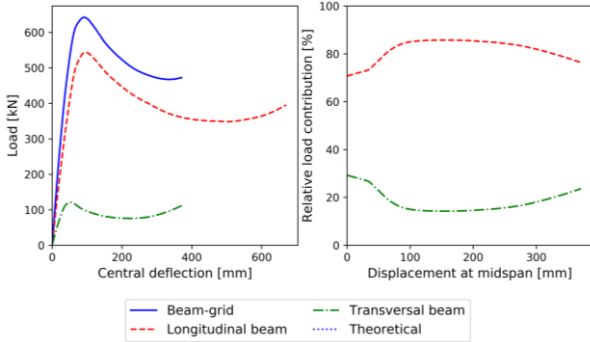


Figure 3. Load-deflection behavior (left) and load redistribution (right) of the reference beam-grid with an aspect ratio γ of 0.5 and relative slenderness λ of 12.

As can be seen in Figure 3 the load bearing capacity of the beam-grid and longitudinal beam is governed by compressive membrane action. Although a high ductility class was selected for the reinforcement steel, it seems that no tensile membrane action can be developed for this reference beam-grid. However for the individual transversal beam, more tensile membrane action develops. As the length of the transversal beam is half of the length of the longitudinal beam and the relative slenderness of both beams is kept equal, the height of the transversal beam is half of the height of the longitudinal beam (see equation 3). Subsequently the reduction in beam height reduces compressive membrane action and enhances the rotation capacity of the beam which in turn increases tensile membrane action. In Figure 3 also the theoretical load-deflection curve is shown which is composed of the sum of the individual load-deflection curve of the longitudinal and transversal beam, and perfectly coincides with the numerical load-deflection curve of the beam-grid. As a consequence it can be concluded that one can take the sum of the load-deflection curve of the individual beams to estimate the load-deflection curve of a beam-grid subjected to a central support removal. On the contrary it should be noted that the ultimate load bearing capacity of the beam-grid is not equal to the sum of the ultimate load bearing capacities of the individual beams. As the load bearing capacities of the individual beams do not

occur at the same central deflection, taking the sum of the ultimate load bearing capacities would overestimate the ultimate load bearing capacity of the beam-grid.

As illustrated in the right part of Figure 3, in general the longitudinal beam has the largest contribution to the load bearing capacity of the beam-grid. Still the load redistribution between the longitudinal beam and transversal beam is not constant for the complete load-deflection curve of the beam-grid. At low deflections, the contribution of the longitudinal beam is increasing due to the development of significant compressive membrane action in this beam. At larger deformations on the other hand the contribution of the transversal beam is increasing due to tensile membrane action. The development of membrane forces in the beam-grid are presented in Figure 4. As expected larger compressive membrane forces are found for the longitudinal beam than for the transversal beam. For the transversal beams at large central deflections, the tensile membrane phase has been initiated. The longitudinal beam on the other hand is still in the transient phase when the beam-grid fails.

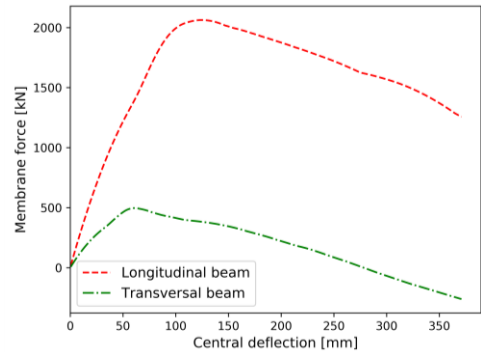


Figure 4. Development of membrane forces in the reference beam-grid with an aspect ratio γ of 0.5 and relative slenderness λ of 12.

In case the height of the transversal beam is kept equal to the height of the longitudinal beam (i.e. approach 2) a different behavior is observed. In the left of Figure 5 the load-deflection curve is shown for the reference beam-grid with an aspect ratio γ of 0.5 and a constant beam height of 500 mm (i.e. $\lambda_{long} = 12$ and $\lambda_{trans} = 6$). In this case significant compressive membrane action develops in the transversal beam due to the increased beam height. As a consequence the contribution of the transversal beam governs the load bearing capacity

of the beam-grid (Figure 5 (right)). At larger vertical deflections, i.e. after the occurrence of the load bearing capacity peak by compressive membrane action, the contribution of the transversal beam decreases and the contribution of the longitudinal beam increases.

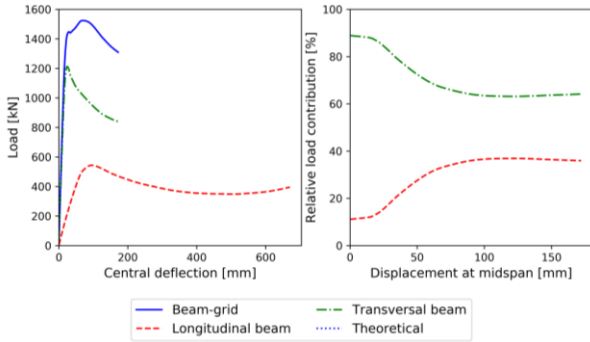


Figure 5. Load-deflection behavior (left) and load redistribution (right) of the reference beam-grid with an aspect ratio γ of 0.5 and constant beam height of 500 mm.

In Figure 6 the development of the membrane forces is presented for the reference beam-grid with an aspect ratio γ of 0.5 and a constant beam height of 500 mm. In this case both beams develop significant compressive membrane forces. Further both beams are still in the transient phase when failure of the beam-grid occurs.

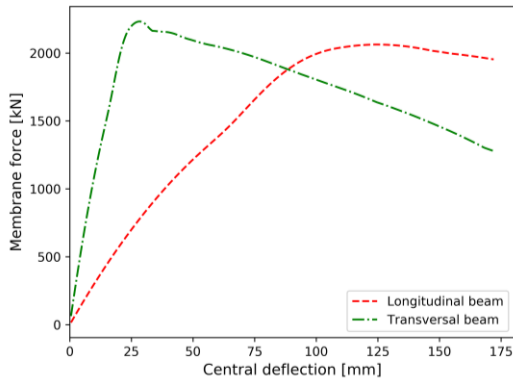


Figure 6. Development of membrane forces in the reference beam-grid with an aspect ratio γ of 0.5 and constant beam height of 500 mm.

Despite the difference in the load redistribution, for both reference models failure of the transversal beam governs failure of the beam-grid. Due to the smaller span length of the transversal beam, for the same central deflection larger rotations occur at the clamped support, resulting in rupture of the reinforcement.

6 Results of parametric studies

6.1 Influence of the aspect ratio

One of the main influencing factors on the load redistribution mechanisms of a beam-grid subjected to a central support removal is the aspect ratio γ . Hence in this section the aspect ratio γ of the reference beam-grid is varied between 0.5 and 1.0. Smaller values than 0.5 are not chosen as in this case it is believed that the loads will be redistributed in one main direction. In Figure 7 the load-deflection curves and relative load contribution diagrams are illustrated for beam-grids with different aspect ratios and with a constant relative slenderness λ of 12 (i.e. approach 1). Similarly Figure 8 shows the load-deflection curves and relative load contribution diagrams in case of a constant beam height for the longitudinal and transversal beam (approach 2). The dimensions of the transversal beam in function of the aspect ratio of the beam-grid for both approaches are given in Table 6.1.

Table 6.1. Dimensions transversal beam in function of the aspect ratio of the beam-grid.

| γ [-] | $l_{trans,init.}$ [mm] | Approach 1 | | Approach 2 | |
|-----------------|---------------------------|---------------------|--------------------------|---------------------|--------------------------|
| | | h_{trans} [mm] | λ_{trans} [-] | h_{trans} [mm] | λ_{trans} [-] |
| 0.5 | 3000 | 250 | 12 | 500 | 6 |
| 0.7 | 4200 | 350 | 12 | 500 | 8.4 |
| 1.0 | 6000 | 500 | 12 | 500 | 12 |

As expected, from Figure 7 and Figure 8 it can be seen that in case the aspect ratio γ of the beam-grid tends to 1, the loads are distributed more equally between the longitudinal and transversal beam. In case the slenderness of the beams is kept constant, increasing the aspect ratio of the beam-grid increases the load bearing capacity. On the contrary in case the beam height of the longitudinal and transversal beam is kept equal, increasing the aspect ratio, decreases the load-bearing capacity of the beam-grid. This observed difference can be explained by the following reasoning. For the first approach (constant relative slenderness), an increase of the aspect ratio will result in an increase of the transversal beam height which enhances the compressive membrane action. For the second approach (constant beam height), an increase of the aspect ratio will result in an increase of the

relative slenderness of the transversal beam which decreases the compressive membrane action and consequently the load bearing capacity of the beam-grid.

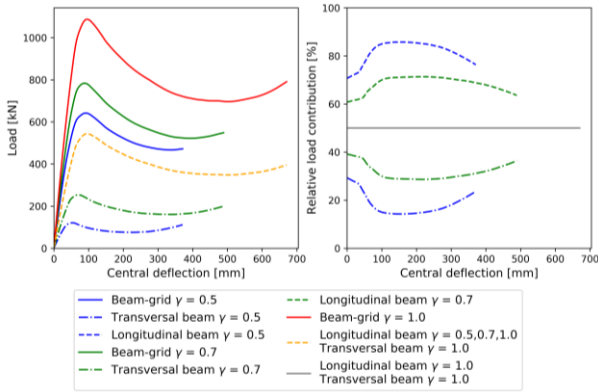


Figure 7. Influence of the aspect ratio γ on the load-deflection behavior (left) and load redistribution (right) of the reference beam-grid with a relative slenderness λ of 12.

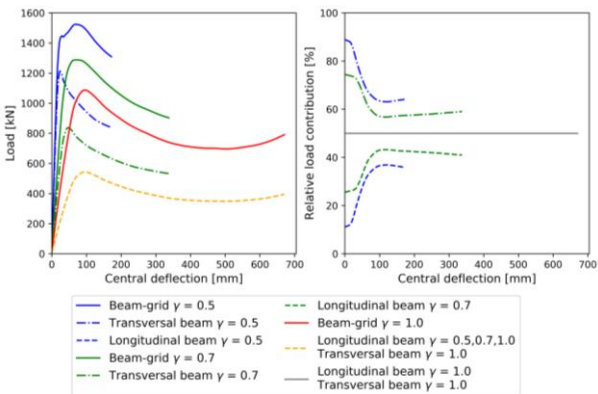


Figure 8. Influence of the aspect ratio γ on the load-deflection behavior (left) and load redistribution (right) of the reference beam-grid with a constant beam height of 500 mm.

6.2 Influence of the reinforcement ratio

In this section the influence of the reinforcement ratio of the beams on the load-deflection behavior and load redistribution is investigated. As such the reinforcement ratio of the reference beam-grid with an aspect ratio γ of 0.5 and a relative slenderness λ of 12 is varied between 0.005 and 0.02. The influence of the reinforcement ratio on the load-deflection behavior is presented in Figure 9. As expected increasing the reinforcement ratio enhances the load bearing capacity of the beam-grid. An increase of the reinforcement ratio mainly enhances the bending strength of the beams and

consequently improves the load bearing capacity due to compressive membrane action as well. Further, for larger reinforcement ratios more tensile membrane action is developed. Nonetheless, for the considered reference case the load bearing capacity is still governed by compressive membrane action for a reinforcement ratio of 0.02.

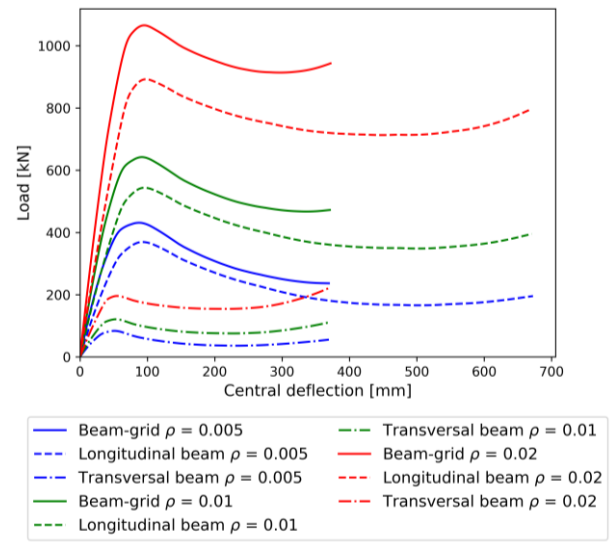


Figure 9. Influence of the reinforcement ratio on the load-deflection behavior of the reference beam-grid with an aspect ratio γ of 0.5 and relative slenderness λ of 12.

6.3 Influence of the ultimate reinforcement strain

In order to enhance the development of tensile membrane action in the reference beam-grid with an aspect ratio γ of 0.5 and a slenderness λ of 12, the ultimate reinforcement strain ϵ_{su} is increased to 12.5 % and 15 %. The resulting load-deflection curves and load redistributions are compared in Figure 10 to the reference beam-grid with an ultimate reinforcement strain of 9.18 %. Similarly to the observations on individual reinforced concrete beams, increasing the ultimate reinforcement strain greatly improves the deformation capacity of the system. Consequently the development of tensile membrane action is enhanced. Still, despite the considered large ultimate reinforcement strain for the reference beam-grid, the ultimate load bearing capacity is still governed by compressive membrane action due to the limited rotation capacity of the individual beams. Further, from the load redistribution diagram (Figure 10, right) it can

be concluded that for larger central deflections where tensile membrane action is governing, the loads will be redistributed more evenly between the longitudinal and transversal beam. Due to the large deformations and as both beams have the same reinforcement ratio, a catenary net will form for the two beams for which the loads are more equally distributed.

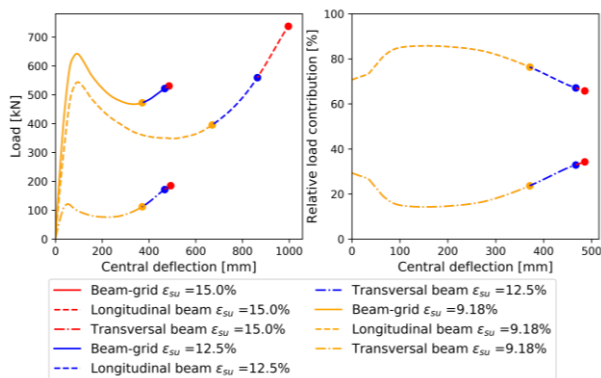


Figure 10. Influence of the ultimate reinforcement strain ϵ_{su} on the load-deflection behavior (left) and load redistribution (right) of the reference beam-grid with an aspect ratio γ of 0.5 and relative slenderness λ of 12.

7 Discussion

In relation to the previous analyses, the following remarks should be made:

- The numerical model does not include possible 3D contribution effects of slabs in redistributing the acting loads.
- Dynamic effects which may be involved with the notional column removal are not taken into account.
- Previous results are based on a case-specific study. Hence, the results should be treated as indicative only.
- In this contribution only a symmetric damage situation (support removal) was considered. Further research should be conducted to investigate non-symmetric damage situations for which the beams are not intersecting at mid-span.

8 Conclusion and recommendations

As limited information is available regarding the load redistribution mechanisms in reinforced concrete beam-grids subjected to a central support removal, numerical analyses are performed in this

contribution. Further, for each analyzed beam-grid separate analyses were also executed for the longitudinal and transversal beam in order to get a better insight in the different load redistribution mechanisms. Two different design approaches and various design parameters were considered to assess their influence on the load redistribution mechanism. In case the slenderness of the beam-grid was kept constant for the longitudinal and transversal beam, it was found that the compressive membrane action of the longitudinal beam governed the load bearing capacity of the beam-grid. On the contrary if the heights of the longitudinal beam and transversal beam were equal, the compressive membrane action of the transversal beam was governing. Still, for both beam-grid designs compressive membrane action was governing and no significant tensile membrane action could be developed due to the limited rotation capacity of the beams. Further for both design approaches failure was governed by rupture of the reinforcement of the shortest beam. As a consequence, special attention should be given to the ductility and deformation capacity of the shortest spans in a beam-grid in order to improve the structural integrity by applying prescriptive ties.

Despite all nonlinear effects related to large deformations and deflections when a central support is removed in a RC beam-grid, taking the sum of the load-deflection curve of the individual longitudinal and transversal beam results exactly in the load-deflection curve of the beam-grid. Nonetheless, taking the sum of the ultimate load bearing capacity of the longitudinal and transversal beam, will result in an overestimation of the ultimate load bearing capacity of the beam-grid, as the longitudinal and transversal beam do not attain their ultimate load bearing capacity at the same deflection. Only in case the aspect ratio γ of the beam-grid is 1, taking the sum of the ultimate load bearing capacities will give a correct estimate. As shown by a parametric study, in case the aspect ratio γ of the beam-grid tends to 1, the load will also be redistributed more equally between the longitudinal and transversal beam. Adding additional reinforcement to the beam-grid greatly enhances the load bearing capacity of the beam-grid as this improves the bending capacity of the individual beams. However even for a large reinforcement ratio no tensile membrane action

could be developed for the considered reference beam-grid. Also for an increased ultimate reinforcement strain of 15 % no tensile membrane action could be developed due to the limited rotation capacity of the beams. Whereas the analyses were based on a beam-grid subjected to a central point-load, the conclusions can be generalized for beam-grids subjected to uniform loads.

9 Acknowledgements

The authors wish to thank Ghent University for the financial support from the Special Research Fund (BOF) on the research project “Risk and reliability-based evaluation and development of design guidelines for structural robustness measures in constructions taking into account membrane action”.

10 References

- [1] J. Agarwal, M. Haberland, M. Holický, M. Sykora, and S. Thelandersson, “Robustness of Structures: Lessons from Failures,” *Struct. Eng. Int.*, vol. 22, no. 1, pp. 105–111, Feb. 2012.
- [2] B. R. Ellingwood, “Mitigating Risk from Abnormal Loads and Progressive Collapse,” *J. Perform. Constr. Facil.*, vol. 20, no. 4, pp. 315–323, 2006.
- [3] D. Gouverneur, R. Caspeele, and L. Taerwe, “Experimental investigation of the load–displacement behaviour under catenary action in a restrained reinforced concrete slab strip,” *Eng. Struct.*, vol. 49, pp. 1007–1016, Apr. 2013.
- [4] H. S. Lew, Y. Bao, S. Pujol, and M. A. Sozen, “Experimental Study of Reinforced Concrete Assemblies under a Column Removal Scenario,” *ACI Struct. J.*, vol. 111, no. 4, pp. 881–892, Jul. 2014.
- [5] J. Yu and K. H. Tan, “Structural Behavior of RC Beam-Column Subassemblages under a Middle Column Removal Scenario,” *J. Struct. Eng.*, vol. 139, no. 2, pp. 233–250, Feb. 2013.
- [6] K. Qian and B. Li, “Experimental and Analytical Assessment on RC Interior Beam-Column Subassemblages for Progressive Collapse,” *J. Perform. Constr. Facil.*, vol. 26, no. 5, pp. 576–589, Oct. 2012.
- [7] K. Qian, B. Li, and J. Ma, “Load-Carrying Mechanism to Resist Progressive Collapse of RC Buildings,” *J. Struct. Eng.*, vol. 141, no. 2, p. 04014107, 2014.
- [8] X. Lu, K. Lin, Y. Li, H. Guan, P. Ren, and Y. Zhou, “Experimental investigation of RC beam-slab substructures against progressive collapse subject to an edge-column-removal scenario,” *Eng. Struct.*, no. August, 2016.
- [9] Pacific Earthquake Engineering Research Center Univ. of California, “OpenSEES.” Research Center Pacific Earthquake Engineering California, Univ. of, Berkeley, CA, 2007.
- [10] Y. Bao, S. K. Kunnath, S. El-Tawil, and H. S. Lew, “Macromodel-Based Simulation of Progressive Collapse: RC Frame Structures,” *J. Struct. Eng.*, vol. 134, no. 7, pp. 1079–1091, 2008.
- [11] A. Fascetti, S. K. Kunnath, and N. Nisticò, “Robustness evaluation of RC frame buildings to progressive collapse,” *Eng. Struct.*, vol. 86, 2015.
- [12] A. H. Arshian, G. Morgenthal, and S. Narayanan, “Influence of modelling strategies on uncertainty propagation in the alternate path mechanism of reinforced concrete framed structures,” *Eng. Struct.*, vol. 110, pp. 36–47, Mar. 2016.
- [13] W. Botte, D. Gouverneur, R. Caspeele, and L. Taerwe, “Influence of Design Parameters on Tensile Membrane Action in Reinforced Concrete Slabs,” *Struct. Eng. Int.*, vol. 25, no. 1, pp. 50–60, Feb. 2015.
- [14] CEN, “Eurocode 2 - Design of concrete structures - Part 1-1: General rules and rules for buildings (+AC:2010),” Brussels (Belgium), 2005.
- [15] D. Droogné, W. Botte, and R. Caspeele, “A multilevel calculation scheme for risk-based robustness quantification of reinforced concrete frames,” *Eng. Struct.*, vol. 160, no. May 2017, pp. 56–70, 2018.